Articles

Journal of Avian Biology 48: 872–880, 2017
doi: 10.1111/jav.01313

Subject Editor: Theresa Burg. Editor-in-Chief: Jan-Åke Nilsson. Accepted 21 December 2016

Ultraconserved elements resolve the phylogeny of potoos (Aves: Nyctibiidae)

Noor D. White, Charles Mitter and Michael J. Braun

N. D. White (http://orcid.org/0000-0002-9510-3744) (noordwhite@gmail.com) and M. J. Braun, Dept of Vertebrate Zoology, National Museum of Natural History, Smithsonian Inst., Washington, DC, USA. – NDW, MJB, and C. Mitter, Behavior, Ecology, Evolution and Systematics Graduate Program, Univ. of Maryland, College Park, MD, USA. CM also at: Dept of Entomology, Univ. of Maryland, College Park, MD, USA.

In this study, we apply a genome-scale set of molecular markers, ultraconserved elements, to fully resolve the phylogeny of a family of secretive, nocturnal birds, the potoos (Nyctibiidae). This dataset provides an opportunity to explore some challenges of phylogenetic analyses of genome-scale datasets, which we address in several ways. We generate data matrices ranging between 2610–4175 loci (1 477 319–3 848 295 aligned base pairs) that represent versions of the data differing in whether or not alignments were trimmed prior to concatenation, and whether 100 or 75% of all taxa were required to be represented by data for inclusion of a given locus. These matrices are analyzed with both maximum likelihood and coalescent algorithms, to check for artifacts of concatenation. Then, we subsample our data matrix by locus into randomly-selected replicates of 125–1000 loci, and compare the topologies and statistical support of the resulting trees to look for evidence of systematic error. In analyses of complete matrices, we find strong statistical support for all ingroup nodes of the tree with no evidence for systematic error introduced by alignment trimming, missing data, or concatenation. We find further support for that topology in our subsampling analyses and statistical topology tests. The earliest branch of the tree separates *Nyctibius bracteatus* from the rest of the potoos, followed successively by *N. grandis* and *N. aethereus.* Two pairs of species, *N. jamaicensis* plus *N. griseus*, and *N. leucopterus* plus *N. aethereus* comprise the distal tips of the tree. Finally, we compare our strongly supported topology to those of previous studies, and use the phylogeny to examine the evolutionary history of potoos.

The family Nyctibiidae, the potoos, consists of seven currently recognized species, subdivided into 15 subspecies (Cohn-Haft 1999, Cohn-Haft 2016, Remsen et al. 2016). Potoos are part of a radiation of nocturnal birds including the nightjars, nighthawks, oilbird, frogmouths, owlet-nightjars and allies. The diurnal clade Apodiformes (swifts and hummingbirds) is embedded within this radiation, and together they comprise the strongly established clade Strisores (Barrowclough et al. 2006, Ericson et al. 2006, Hackett et al. 2008; reviewed by Braun and Huddleston 2009).

Like most other nocturnal birds of this group, potoos rest during the day, protected by their cryptic coloration and body form, and forage for insects at night (Cohn-Haft 1999). Also like other nightbirds, they show adaptations for night vision, including possession of a tapetum lucidum (reviewed by Braun and Huddleston 2009). They differ from most other nightbirds in lacking rictal bristles around the beak, having a 'toothed' bill, and possessing notches in their upper eyelids, which are thought to allow some vision during the day without revealing their bulbous eyes to potential predators (Borrero 1974, Cohn-Haft 1999). Most species of potoos are also known for perching upright at the end of dead snags, assuming a cryptic pose in which they bear a remarkable resemblance to the snag itself. Some descriptions even suggest that their plumage patterns resemble lichens growing on dead wood, enhancing their camouflage (Cohn-Haft 1999). This posture is similar to one taken by some species of frogmouths (family Podargidae), which are currently restricted to the Old World.

The current distribution of Nyctibiidae is entirely Neotropical, although the fossil record suggests that they were previously more widespread (Mayr 2005a, b). Several species overlap extensively in geographic range (Fig. 1). Potoos primarily inhabit lowland moist forest except for *Nyctibius maculosus*, which is found in montane moist forest. The potoos are conservative in external appearance, and plague systematists with their cryptic coloration and high degree of individual variation. Some species boundaries are based largely on differences in vocalizations, such as that between the common *Nyctibius griseus* and northern *Nyctibius jamaicensis* potoos. However, genetic divergence among potoos is high, suggesting that these species are quite old, despite their conservative morphology. For example, mitochondrial cytochrome b (MT-CYB) sequence divergence ranges from 11.1–16.2% in potoos (Mariaux and

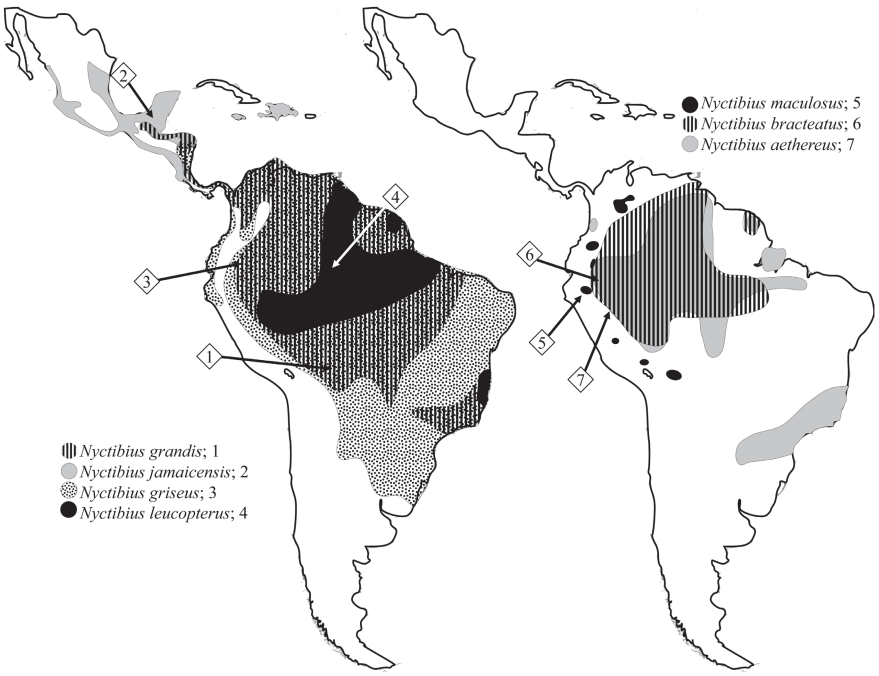

Figure 1. Maps of Central and South America depicting geographic distributions of potoo species. Range maps based on Cohn-Haft (2016). Collection localities of specimens used in this study are indicated by numbered arrows.

Braun 1996), greatly exceeding the range of ~1–10% more typically observed among congeneric bird species (Brumfield et al. 1997, Braun and Huddleston 2009).

A strongly resolved phylogeny, prerequisite for understanding the contrasting patterns of phenotypic and genetic diversity within *Nyctibius*, is not yet available. The first molecular study, based on partial MT-CYB sequences, was unable to fully resolve relationships among the six species sampled, but did suggest that *Nyctibius leucopterus* and *N. maculosus* are sister taxa (Mariaux and Braun 1996; Fig. 2). Allozyme data subsequently confirmed the grouping of *N. leucopterus* and *N. maculosus*, additionally finding that *N. griseus* is probably sister to that pair, and that *N. bracteatus* is likely sister to all other potoos (Brumfield et al. 1997; Fig. 2). In an analysis of all seven species based on combining data from MT-CYB with the cellular homolog of the myelocytomatosis viral oncogene (MYC; 2274 bp total), Braun and Huddleston (2009) found strong support for the pairing of *N. griseus* with *N. jamaicensis*, and *N. leucopterus* with *N. maculosus*, but only weak evidence regarding the remaining relationships (Fig. 2). The most recent study of potoo relationships firmly places *Nyctibius bracteatus* as sister to all other potoos

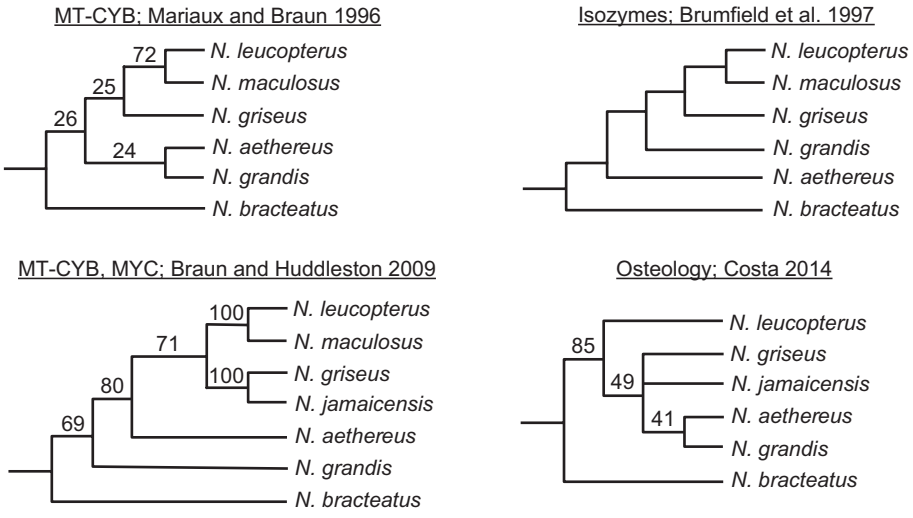

Figure 2. Cladograms of previous estimates of potoo phylogeny. Data used for each study is shown in the labels. MT-CYB = mitochondrial cytochrome b; MYC = cellular homolog of the myelocytomatosis viral oncogene. Where available, bootstrap support is depicted. The isozyme tree of Brumfield et al. (1997) is from Fig. 2B of that paper.

based on osteological evidence, but lacks strong resolution of the rest of the taxa (Costa 2014; Fig. 2).

In this study, we established a robust phylogeny for potoos using ultraconserved elements (UCEs; Faircloth et al. 2012, McCormack et al. 2012). The advent of high-throughput DNA sequencing technology (also referred to as 'next generation' or 'massively parallel') has enabled the rapid generation of genome-scale datasets. In the present case, the size of our UCE dataset represents a roughly hundred-fold increase over the most recent study of potoo phylogeny (Braun and Huddleston 2009). The extraordinary information content of these genome-scale molecular matrices has allowed for unprecedented resolution of phylogenetic relationships, but has also brought to light new issues in data analysis. These issues are particularly problematic when they are due to systematic error – errors that give increasing statistical confidence in the wrong answer when increasing amounts of data are analyzed (Kumar et al. 2012, Hahn and Nakhleh 2015, Hosner et al. 2016). The possible artifacts most relevant to our dataset and the phylogeny in question are the effect of trimming sequence alignments, discussed by Capella-Gutierrez et al. (2009), and the effect of missing data, discussed by Hosner et al. (2016).

The information content of UCEs comes largely from the flanking regions that are captured as a result of targeting the ultra-conserved core. Trimming of UCE loci after alignment is potentially a double-edged sword in that trimming away the 'ragged' ends of alignments should reduce phylogenetic error due to sequence error or poor alignment, but possibly at the cost of losing informative sequence. Trimming algorithms were originally introduced to compensate for any potential noise introduced at the ends of alignments. These regions generally represent areas of lower sequencing coverage, and thus more sequencing error. These regions are also more difficult to align due to variation in sequence lengths across taxa. In the past, alignments were checked by eye to remove any potentially mis-aligned regions that could include non-homologous characters. However, this is not possible with a genome-scale dataset, and thus we rely on computational methods to scan alignments for us. Potential artifacts due to missing data are another concern in phylogenomic analysis (Hosner et al. 2016). A recent study applying UCEs to lizards found that varying matrix completeness (where completeness refers to percentage of taxa for which data are available for a given locus) can affect support for inferred relationships, and that maximum likelihood analyses of concatenated datasets benefitted from the inclusion of more genes, even though missing data increased (Streicher et al. 2015). Thirdly, high overall bootstrap support in genome-scale datasets can mask strong conflicts among loci or groups thereof, which might suggest lower confidence in the total evidence tree (Salichos and Rokas 2014). One indicator of the existence of strong conflict would be marked variation in topology and support among trees built from subsets of loci.

Here, we gauged the impact of these potential artifacts on our results in several ways. We constructed datasets with varying levels of missing data and analyzed them before and after trimming. To look for conflict among loci or groups thereof, we randomly subsampled our loci, and compared the resulting trees. This exercise also enabled us to estimate the minimum number of loci required to find the total evidence tree with strong support. Having detected no evidence for artifacts (i.e. systematic error) due to analyzing genome-scale matrices, we compare our results to those of previous studies, and use the phylogeny to examine the evolutionary history of potoos.

Material and methods

Taxon sampling

Taxon sampling for this study consisted of all seven currently recognized potoo species plus five representatives of the other major lineages of Strisores (one individual each, 12 species total; Table 1). Frozen tissue samples were assembled through our own fieldwork and loans from major museum collections. Purified DNA samples were available from our previous work on these species (Hackett et al. 2008, Braun and Huddleston 2009).

Data collection and alignment

UCE data were collected by sequence capture using the tetrapod probe set of Faircloth et al. (2012), following the laboratory protocols described in that paper and available at <www.ultraconserved.org>. This probe set is designed to enrich sequencing libraries for 5060 UCE loci conserved across tetrapods. Sequencing of paired-end, 100 base pair (bp) reads was conducted on Illumina platforms (HiScan and HiSeq2000), recovering an average of 1 456 836 reads per species (600 814–2 995 105). Sequences were processed with the PHYLUCE software package (Faircloth 2016) including quality control, assembly using Velvet (ver. 1.2.09; Zerbino 2008) and matching of contigs to UCE locus probes using LASTZ (Harris 2007). Individual loci were aligned using SATé-II based on MAFFT (ver. 2.2.7; Liu et al. 2011).

Matrix completeness, alignment trimming and subsampling of loci

To test the effect of missing data, we generated two datasets varying in 'matrix completeness', a term we use to refer to the proportion of taxa represented for a given locus. In one dataset, every taxon is represented in every locus alignment (termed '100% complete'), while the other dataset has at least 75% of all taxa represented for every locus ('75% complete'). For the purposes of this study, 75% completeness represented a threshold where we could both test the effects of missing data by introducing a lot of loci (nearly doubling the dataset relative to 100% complete) where one or more taxa were not represented, but also maintain computational tractability for the variety of analyses we wanted to run.

For each of these datasets, we also subjected individual locus alignments to the trimming algorithm included in the PHYLUCE software in order to test the effect of alignment trimming on phylogenetic inference. The PHYLUCE trimmer parses a given alignment in 20 bp windows, removing 'ragged' ends, so that at least 65% of taxa are present in a given column, and at least 65% of residues are present within

Table 1. Collection details for all specimens used in this study. Localities appear as given in their respective collection databases. Abbreviations: ABTC = Australian Biological Tissue Collection (South Australian Museum, Adelaide); ANSP = Academy of Natural Sciences, Philadelphia; ANWC = Australian National Wildlife Collection, Canberra; FMNH = Field Museum of Natural History, Chicago; KUNHM = Univ. of Kansas Natural History Museum, Lawrence; LSUMZ = Louisiana State Univ. Museum of Zoology, Baton Rouge; WLK = preparator L. K. Wang; UWBM = Univ. of Washington, Burke Museum, Seattle; SAMA = South Australian Museum, Adelaide.

Common name	Species	Tissue no.	Voucher no.	Locality	Collector
Long-tailed potoo	*Nyctibius aethereus*	LSUMZ B10877	LSUMZ 156210	Peru; Depto Ucayali, SE slope of Cerro Tahuayo	A. S. Meyer
Rufous potoo	*Nyctibius bracteatus*	LSUMZ B4509	LSUMZ 114641	Peru; Depto Loreto, lower Rio Napo region, E bank of Rio Yanayacu, ~90 km N of Iquitos	S. W. Cardiff
Great potoo	*Nyctibius grandis*	LSUMZ B15415	LSUMZ 150545	Bolivia; Depto Santa Cruz, Velasco, Pre-Parque Nacional: 'Noel Kempff Mercado', 30 km E of Aserradero Moira	J. M. Bates
Common potoo	*Nyctibius griseus*	ANSP 18217 (B3238)	ANSP 183090	Ecuador; Prov. Sucumbios, Imuya Cocha 0°34'S, 75°17'W, 200 m	F. Sornoza
Northern potoo	*Nyctibius jamaicensis*	KUNHM 2116	KUNHM 92957	Mexico; Silvituc, 24 km S; Mexico, Campeche; 18.233, –90.200	–
White-winged potoo	*Nyctibius leucopterus*	LSUMZ B20315	LSUMZ 165693	Brazil; Amazonas, Munic. Manaus; km 34 ZF-3, Faz. Esteio, ~80 km N of Manaus	M. Cohn-Haft
Andean potoo	*Nyctibius maculosus*	LSUMZ B271	LSUMZ 97586	Peru; Depto Cajamarca, Lucuma on the Sapalache-Carmen Trail	M. J. Braun
Oilbird	*Steatornis caripensis*	LSUMZ B32579	LSUMZ 169580	PERU; Cajamarca Region	R. C. Faucett
Philippine frogmouth	*Batrachostomus septimus*	FMNH 429205	FMNH 429205	Philippines; Luzon County, Kalinga 17.4417N, 121.0708E	–
Australian owlet-nightjar	*Aegotheles cristatus*	ABTC 24643	SAMA B39188	Australia; South Australia, 15 km from Lagoon Witt, Mabel Creek	–
Moustached treeswift	*Hemiprocne mystacea*	WLK 385	UWBM 68087	Solomon Islands; New Georgia Island, Arara, 8°29.5'S, 157°38.8'E (-8.492; 157.647)	C. E. Filardi
White-throated nightjar	*Eurostopodus mystacalis*	ANWC B40813	ANWC B40813	Australia; Australian Capital Territory, Canberra, ~35°21'S, 149°058'E	–

that window. For each window, it allows no more than 20% divergence between any row of the alignment and the consensus of all sequences in that window. Lastly, it removes any loci with a trimmed length shorter than 100 bp. Resulting datasets varied from 2610–4175 loci, were ~1.5–3.8 million bp in length, and contained ~43 000–98 000 parsimony informative sites (Table 2).

To test the resolving power of UCE data, we randomly selected subsets of the 100% complete, PHYLUCE-trimmed matrix to create matrices of 125, 250, 500, 750 and 1000 loci. Three replicate matrices of each size were created. These matrices ranged from ~69–572 kilobases in length, and contained ~2000–17 000 parsimony-informative sites (Table 3). All data matrices generated by this study are available in Treebase (ID # 20258).

Phylogenetic analyses

Model selection was conducted using jModeltest 2.1.10 (ver. 20160303; Darriba et al. 2012). A general-time reversible model with estimated proportion of invariant sites and gamma-distributed rate variation among sites (GTR + I + G) was selected as the most appropriate model according to the corrected Akaike information criterion for all our datasets (Akaike 1973, Hurvich and Tsai 1989). Maximum likelihood (ML) phylogenetic analyses of the 100% complete and 75% complete datasets were conducted on concatenated matrices with GARLI (ver. 2.1; Zwickl 2006). One hundred independent runs of the program were conducted, using two search replicates in each run ('searchreps = 2'). We used the 'treedist' function of PAUP* (ver. 4.0a150; Swofford 2003) to ensure that the same topology was found for the best replicate in each of the 100 runs. This method is used as a means of assessing the thoroughness of the search of

Table 2. Number of loci, alignment length (in base pairs), and number of parsimony-informative sites in the full UCE data matrices.

Completeness	Matrix	Loci	Alignment length (bp)	Informative sites
100%	Untrimmed	2610	2 541 839	69 740
	Trimmed	2610	1 477 319	43 571
75%	Untrimmed	4175	3 848 295	98 576
	Trimmed	4174	2 219 207	62 496

Table 3. Number of loci, alignment length (in base pairs), and number of parsimony-informative sites in the UCE subset matrices.

Loci	Replicate	Alignment length (bp)	Informative sites
125	1	71 189	2082
	2	72 700	2003
	3	69 359	2124
250	1	143 882	4527
	2	138 773	3900
	3	140 230	4224
500	1	284 365	8047
	2	281 767	8228
	3	280 130	8111
750	1	425 434	12 613
	2	428 598	12 685
	3	427 130	12 497
1000	1	572 481	16 812
	2	566 594	16 693
	3	568 380	16 663

treespace, and is described in White et al. (2016). To evaluate nodal support, we conducted 100 non-parametric bootstrap replicates, each with one search replicate. The relatively small number of taxa in this dataset (n = 12) enabled us to run tree searches guaranteed to find the optimal topology. We ran both branch and bound and exhaustive tree searches in PAUP* (ver. 4.0a150; Swofford 2003) under GTR + I + G, and the resulting topologies were identical to that found by GARLI, ensuring that we have found the optimal tree.

ML analyses of the randomly subsampled matrices were conducted using both RAxML (ver. 8.2.7; Stamatakis 2014) and GARLI (ver. 2.1; Zwickl 2006), under the GTR + I + G model. In RAxML, searches for the best topology consisted of 20 replicates, and bootstraps were run using the bootstopping criterion (option – 'autoMRE'). In GARLI, searches for the best topology consisted of 100 independent runs of 2 search replicates each, and 100 non-parametric bootstraps (one search replicate each) were run.

To test for the possibility that gene tree/species tree discordance introduces artifacts in our concatenated analyses, we applied a coalescent-based species tree method, SVDquartets (Chifman and Kubatko 2014, 2015). We employed the SVDquartets code implemented in PAUP* (ver. 4.0a150; Swofford 2003), evaluating all possible quartets and conducting 100 non-parametric bootstrap replicates.

In all cases, bootstrap values were plotted on the optimal topology using the SumTrees program (ver. 4.0.0) in the python library DendroPy (ver. 4.0.2; Sukumaran and Holder 2010). All trees generated in this study were rooted to the Strisores outgroups and have been deposited in Treebase (ID no. 20258).

Topology tests

We employed a statistical topology test to assess the significance in likelihood score of our preferred tree over all plausible trees. To make the search computationally tractable, we constructed a plausible set of trees that incorporates *a priori* information on potoo phylogeny presented in Fig. 2, including the grouping of *N. leucopterus* with *N. maculosus*, as well as *N. griseus* with *N. jamaicensis*. *Nyctibius leucopterus* and *N. maculosus* form a sister clade in all prior analyses, and *N. jamaicensis* was previously classified as a subspecies of *N. griseus*, so these groupings are justified. We also fixed the positions of all outgroup nodes except for *Steatornis caripensis* and *Eurostopodus mystacalis*, again based on prior knowledge (Barrowclough et al. 2006, Hackett et al. 2008, Prum et al. 2015). We devised a constraint tree reflecting these known relationships, and used the constraint topology to generate all plausible dichotomous trees in PAUP* (ver. 4.0a150; Swofford 2003), resulting in 315 candidate topologies. To test the significance of differences in likelihood among trees, we used the approximately unbiased (AU) test of Shimodaira (2002), which is less biased against rejection than the Shimodaira–Hasegawa test (Shimodaira and Hasegawa 1999), and was deemed valid for our application. The AU test was run in PAUP* (ver. 4.0a150; Swofford 2003) using resampling of estimated log likelihoods (RELL) to generate 1000 bootstraps. Tests were run for each of our four full matrices.

Results and discussion

Matrix completeness, alignment trimming and subsampling of loci

PHYLUCE trimming had little effect on the number of loci included (only one locus was eliminated, in the 75% complete matrix), but total alignment length was reduced by about 40%. This reduction had no apparent effect, however, on the phylogenetic result. In each case, the trimmed and untrimmed matrices yielded the same topology, with 100% bootstrap support for every ingroup node in the ML analyses, and a minimum of 98% in the coalescent analyses (Fig. 3, 4). Matrix completeness similarly had no discernable effect on the phylogeny. The 75% complete matrices include

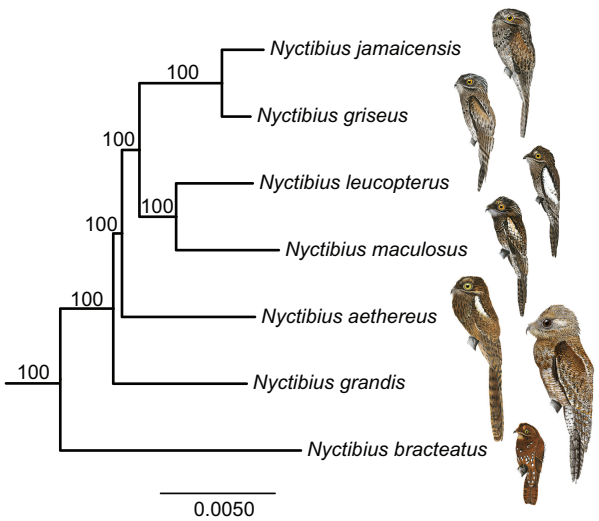

Figure 3. Maximum likelihood phylogram of potoo relationships from GARLI analyses of four UCE datasets (100% and 75% complete, trimmed and untrimmed). Bootstrap support values were 100% for all nodes in all analyses. Branch lengths are from the 100% complete, trimmed dataset. Outgroups not shown. Scale units are substitutions per site. Potoo illustrations represent closest geographic form to specimen used available in Cohn-Haft (2016), and are roughly scaled to size.

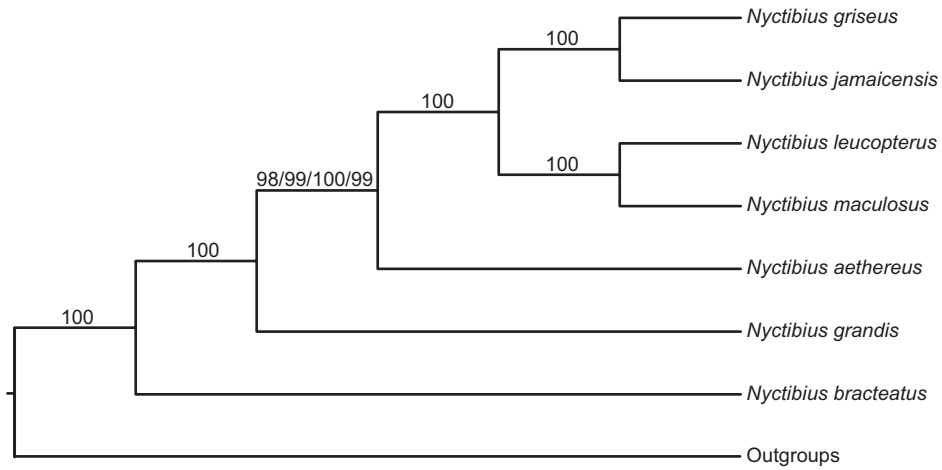

Figure 4. SVDquartets topology with bootstrap support from analyses of 4 datasets as follows: 100% complete, trimmed/100% complete, untrimmed/75% complete, trimmed/75% complete, untrimmed. Outgroups are collapsed.

~1.5 times as many loci as the 100% complete datasets, yet both yielded the same topology with extremely high bootstrap support for every ingroup node in both ML and coalescent analyses. Thus, we find no evidence that our results are sensitive to possible artifacts of alignment trimming or missing data, nor to artifacts of concatenation.

The random subset matrix trees agreed with each other, as well as with those from the complete matrices, with two exceptions. These exceptions represent the other possible resolutions of the trichotomy between *N. aethereus, N. grandis* and a clade of four small potoos (topologies B and C in Fig. 5). Topology B was optimal for one replicate subset of the smallest sample size (125 loci) and topology C was optimal for one replicate subset of 500 loci (Fig. 5). In neither case was the node conflicting with topology A strongly supported. We originally used RAxML to analyze the subset matrices, and re-ran them with GARLI, which yielded the same topologies and similarly low support (Fig. 5). The results indicate that the alternative topologies reflect differing signals in the subsampled matrices, and not a bias of the software used. In sum, we find no evidence that the 100% bootstrap support for all nodes in the analysis of the full dataset is masking pervasive strong conflict – subsampling of genes generally produced the same topology with diminished signal. Our subsampling results also suggest that substantially fewer loci than the 4175 employed

# of Loci	Replicate	RAxML	GARLI
125	1	Topology B	Topology B
	2	73	73
	3	89	89
250	1	98	99
	2	98	100
	3	90	91
500	1	100	100
	2	Topology C	Topology C
	3	95	95
750	1	98	99
	2	100	100
	3	100	100
1000	1	100	99
	2	98	98
	3	100	100

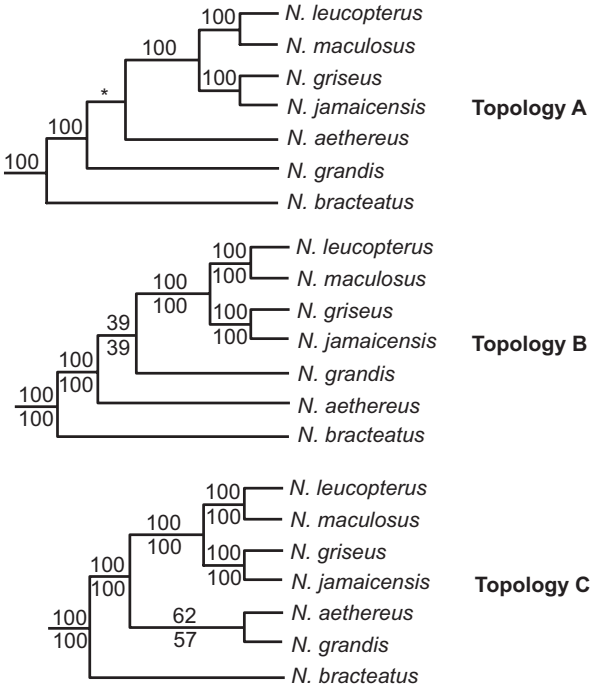

Figure 5. Resolving power of UCE data illustrated by matrix subset tests. Table includes the number of loci in each subset, the replicate number, and the RAxML and GARLI bootstrap support values for the node with an asterisk in topology A. All other nodes had bootstrap support of 100% in all cases. Where indicated, a replicate subset produced topology B or topology C. Bootstrap support values for those topologies are presented for RAxML above branches, and for GARLI below them.

here would suffice to definitively resolve the potoo phylogeny; alternative topologies only appeared with subsets of 500 or fewer loci.

Phylogeny and evolution of potoos

As detailed above, ML and coalescent analyses of genome-scale UCE data yielded a very strongly supported phylogeny of potoos (Fig. 3, 4). The congruence of these two fundamentally different methods enhances confidence in our result. The tree agrees with all strongly supported nodes in previous molecular analyses (Fig. 2), and mirrors that found by Braun and Huddleston (2009), but with much stronger bootstrap support. Our topology differs from that found in the osteological study by Costa (2014), but character support for conflicting nodes in that study is limited. In fact, it would only take one step to make the osteological tree identical to the UCE tree. Specifically, Costa's character 9 requires one more step on the UCE tree, while his character 24 is equally parsimonious on both topologies. We found no evidence for a variety of possible artifacts to which genome-scale datasets are potentially susceptible. AU tests of our four full datasets reject all but 2 or 3 trees (Fig. 6). The trees which cannot be rejected all have the same ingroup topology, which mirrors that found in our ML and coalescent analyses (Fig. 3, 4). We therefore believe that the ingroup topology based on UCE data provides a robust framework for discussion of potoo evolution.

The earliest branch in the potoo tree separates the rufous potoo *N. bracteatus* from all other species. *Nyctibius bracteatus* is arguably the most divergent potoo on several counts. Previous molecular studies all found the highest genetic divergences within potoos to be those between *N. bracteatus* and all other species (Mariaux and Braun 1996, Brumfield et al. 1997). It is the smallest potoo, and bears a unique plumage pattern that more closely resembles the oilbird *S. caripensis* than any of the other potoos. The deeply rufous plumage of *N. bracteatus* is said to mimic dead foliage or dead wood in the forest understory where the species typically nests and roosts during the day, with the white spots resembling dappled sunlight or whitish fungi (Cohn-Haft 1999, B. Whitney pers. comm.). It also has a unique dark wedge in its otherwise yellow iris, the function of which is unknown (Cohn-Haft 1999), and bears a number of unique osteological traits, described in Costa (2014).

Although rarely encountered, *N. bracteatus* appears to be widespread in the tropical lowlands of South America. Behaviorally, it is unique in roosting during the day on thin, roughly horizontal branches, and perpendicular to the substrate, rather than adopting the branch/stub-mimicry roosting posture (frozen with bill up) for which potoos are famous. Furthermore, it is reported to remain in a 'hunched' posture (head down, bill nearly parallel with ground), and to regularly rock back and forth on a vertical axis, assuming the motion of a dead leaf in the breeze (B. Whitney pers. comm.), which may boost blood circulation in this relatively sedentary bird (M. Cohn-Haft pers. comm.). *Nyctibius bracteatus* forages inside forests, principally in the understory, whereas other potoos forage mostly in the canopy and subcanopy, often at forest edges and around larger open clearings within forests (B. Whitney pers. comm.). Lastly, the principal 'song' of *N. bracteatus* is more complex and multi-syllabic than are the presumably homologous songs of other potoos (T. Costa and B. Whitney pers. comm.).

Among the remaining species, the next divergences separate first the great potoo *N. grandis*, then the long-tailed potoo *N. aethereus*, from the others. These two are the largest of the potoos. They are biogeographically similar in having disjunct populations in the Brazilian Atlantic Forest, as well as extensive distributions in lowland tropical South America, including both sides of the Andes. The great potoo is found on the borders of, or in openings in, dry to humid forests, while the long-tailed potoo is restricted to the interior of humid tropical forests.

The final four species form a clade, which divides into two sister-group pairs. One of these consists of the similarly sized white-winged *N. leucopterus* and Andean *N. maculosus* potoos, as first reported by Mariaux and Braun (1996). Both are rarely encountered species of tropical South America. The Andean potoo is unique to the family

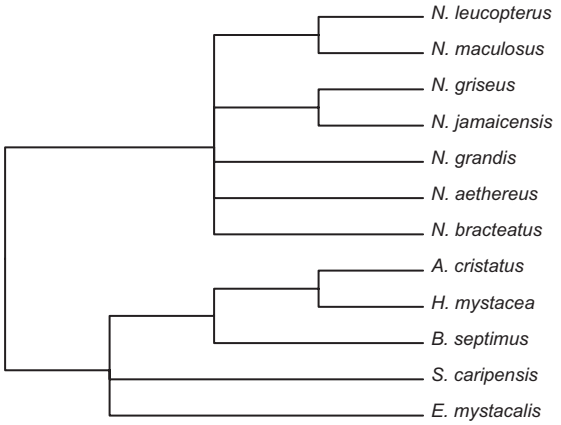

	Tree	-lnL	△ -lnL	p-value
100% complete, trimmed	1	3,308,964.33	(best)	
	2	3,308,968.49	4.16	0.51
100% complete, untrimmed	1	5,842,639.33	(best)	
	2	5,842,775.34	136.01	0.06
75% complete, trimmed	2	4,875,405.89	(best)	
	1	4,875,416.96	11.08	0.55
	3	4,875,518.79	112.90	0.09
75% complete, untrimmed	1	8,633,856.67	(best)	
	2	8,633,983.25	126.58	0.19
	3	8,634,038.05	181.38	0.10

Figure 6. Results of the AU topology test. The constraint tree shown at left implies 315 plausible topologies which must be considered. The resulting likelihood scores (–lnL) are shown for the optimal tree and other trees that cannot be rejected by each of the four full datasets. Difference in likelihood (Δ -lnL) and p-values for suboptimal trees that cannot be rejected are also shown. All other trees had p-values below 0.05. All trees that cannot be rejected had ingroup topologies identical to Fig. 3 and 4, and differed only in the placement of outgroups *S. caripensis* and *E. mystacalis*.

in preferring the habitat of montane cloud forests, whereas the white-winged potoo is a secretive denizen of the canopy of tropical forests. The remaining sister species pair consists of the morphologically similar common *N. griseus* and northern *N. jamaicensis* potoos. Historically *N. jamaicensis* had been treated as a subspecies of *N. griseus*. The two are now split based on their distinct vocalizations. *Nyctibius griseus* has perhaps the broadest distribution of all potoos, ranging over much of South America and into central America as far as Nicaragua. *Nyctibius jamaicensis* occurs in northern central America and on Jamaica and Hispaniola. Both are more commonly encountered than other potoos and may be found in a variety of habitats, from the borders of humid forests and river edges to dry woodlands and open areas.

Given the conserved cryptic plumage of potoos and the high degree of genetic divergence observed in all molecular studies to date, further research on geographic variation in potoos is in order, beginning with previously recognized subspecies and disjunct populations. This would include trans-Andean populations of *N. griseus*, *N. grandis* and *N. aethereus*, and populations of *N. leucopterus*, *N. aethereus* and *N. grandis* isolated in the Atlantic Forest. Research should include studies of molecular, morphological and behavioral (especially vocal) variation, as significant divergence in all of these character suites has been discovered in the examples cited above. While a paucity of traditional museum specimens and genetic resource materials has hampered the study of this elusive group, new technologies such as computed tomography scanning and next generation sequencing promise to facilitate extraction of new information from the specimens that do exist (Lim and Braun 2016).

Of special interest are the island subspecies *N. j. jamaicensis* of Jamaica and *N. j. abbotti* of Hispaniola. Their distributions conform to stage V of the taxon cycle theory (Ricklefs 1970), which would suggest that these populations may be old and substantially divergent from their mainland counterparts. Several other island endemic nightbirds have also proven to be much more divergent than previously suspected. Examples include the Malagasy endemic *Gactornis enarratus* (Han et al. 2010), the Hispaniolan endemic *Siphonorhis brewsteri* (Han et al. 2010) and the Solomon Islands endemic *Rigidapenna inexpectata* (Cleere et al. 2007). *Rigidapenna*, which clearly belongs in a separate genus, was previously treated as a subspecies of *Podargus ocellatus*, and *Gactornis* had always been treated as a species of *Caprimulgus* until molecular data demonstrated that it was one of the oldest lineages of Caprimulgidae.

Acknowledgements – We acknowledge the genetic repositories listed in Table 1 for loans of the tissues used herein. We especially thank the intrepid field collectors and diligent curatorial staff whose work makes studies such as this possible. We thank Thiago V. V. Costa for sharing his unpublished dissertation, Bret Whitney and Mario Cohn-Haft for insight on the behavior and vocalizations of *N. bracteatus*, and Handbook of the Birds of the World for allowing us use of the potoo plate images. Computations in this paper were run on the Smithsonian Institution's High Performance Computing Cluster, Hydra. Laboratory work was conducted at and with the support of the US Natl Museum of Natural History.
Funding – NDW received Smithsonian Inst. support through the Predoctoral Fellowship Program, the Frontiers in Phylogenetics Program, the Scholarly Studies Program and the Consortium for Understanding and Sustaining a Biodiverse Planet.

References

Akaike, H. 1973. Information theory and extension of the maximum likelihood principle. – In: Petrov, B. N. and Csaki, F. (eds). Proc. Second Int. Symp. Inform. Theory, pp. 267–281.

Barrowclough, G. F., Groth, J. G. and Mertz, L. A. 2006. The RAG-1 exon in the avian order Caprimulgiformes: phylogeny, heterozygosity, and base composition. – Mol. Phylogenet. Evol. 41: 238–248.

Borrero, J. I. 1974. Notes on the structure of the upper eyelid of potoos *Nyctibius*. – Condor 76: 210–211.

Braun, M. J. and Huddleston, C. J. 2009. A molecular phylogenetic survey of caprimulgiform nightbirds illustrates the utility of non-coding sequences. – Mol. Phylogenet. Evol. 53: 948–960.

Brumfield, R. T., Swofford, D. L. and Braun, M. J. 1997. Evolutionary relationships among the potoos Nyctibiidae based on isozymes. – Ornithol. Monogr. 48: 129–145.

Capella-Gutierrez, S., Silla-Martinez, J. M. and Gabaldon, T. 2009. trimAl: a tool for automated alignment trimming in large-scale phylogenetic analyses. – Bioinformatics 25: 1972–1973.

Chifman, J. and Kubatko, L. 2014. Quartet inference from SNP data under the coalescent model. – Bioinformatics 30: 3317–3324.

Chifman, J. and Kubatko, L. 2015. Identifiability of the unrooted species tree topology under the coalescent model with time-reversible substitution processes, site-specific rate variation, and invariable sites. – J. Theor. Biol. 374: 35–47.

Cleere, N., Kratter, A. W., Steadman, D. W., Braun, M. J., Huddleston, C. J., Filardi, C. E. and Dutson, G. 2007. A new genus of frogmouth (Podargidae) from the Solomon Islands – results from a taxonomic review of *Podargus ocellatus inexpectatus* Hartert 1901. – Ibis 149: 271–286.

Cohn-Haft, M. 1999. Family Nyctibiidae potoos. – In: del Hoyo, J., Elliott, A. and Sargatal, J. (eds), Handbook of the birds of the world, barn-owls to hummingbirds, vol. 5. Lynx Edicions, pp. 288–301.

Cohn-Haft, M. 2016. Potoos (Nyctibiidae). – In: del Hoyo, J., Elliott, A., Sargatal, J., Christie, D. A. and de Juana, E. (eds), Handbook of the birds of the world alive. Lynx Edicions, <www.hbw.com/node/52264>.

Costa, T. V. V. 2014. Osteology and phylogeny of the avian order Caprimulgiformes, with special emphasis on Nyctibiidae and Caprimulgidae. – PhD thesis, Univ. de São Paulo, São Paulo, Brazil.

Darriba, D., Taboada, G. L., Doallo, R. and Posada, D. 2012. jModelTest 2: more models, new heuristics and parallel computing. – Nat. Methods 9: 772.

Ericson, P. G. P., Anderson, C. L., Britton, T., Elzanowski, A., Johansson, U. S., Kallersjo, M., Ohlson, J. I., Parsons, T. J., Zuccon, D. and Mayr, G. 2006. Diversification of neoaves: integration of molecular sequence data and fossils. – Biol. Lett. 2: 543–547.

Faircloth, B. C. 2016. PHYLUCE is a software package for the analysis of conserved genomic loci. – Bioinformatics 32: 786–788.

Faircloth, B. C., McCormack, J. E., Crawford, N. G., Harvey, M. G., Brumfield, R. T. and Glenn, T. C. 2012. Ultraconserved elements anchor thousands of genetic markers spanning multiple evolutionary timescales. – Syst. Biol. 61: 717–726.

Hackett, S. J., Kimball, R. T., Reddy, S., Bowie, R. C. K., Braun, E. L., Braun, M. J., Chojnowski, J. L., Cox, W. A., Han, K.-L., Harshman, J., Huddleston, C. J., Marks, B. D.,

Miglia, K. J., Moore, W. S., Sheldon, F. H., Steadman, D. W., Witt, C. C. and Yuri, T. 2008. A phylogenomic study of birds reveals their evolutionary history. – Science 320: 1763–1768.

Hahn, M. W. and Nakhleh, L. 2015. Irrational exuberance for resolved species trees. – Evolution 70: 7–17.

Han, K-L., Robbins, M. B. and Braun, M. J. 2010. A multi-gene estimate of phylogeny in the nightjars and nighthawks (Caprimulgidae). – Mol. Phylogenet. Evol. 55: 443–453.

Harris, R. S. 2007. Improved pairwise alignment of genomic DNA. – PhD thesis, The Pennsylvania State Univ., PA, USA.

Hosner, P. A., Faircloth, B. C., Glenn, T. C., Braun, E. L. and Kimball, R. T. 2016. Avoiding missing data biases in phylogenomic inference: an empirical study in the landfowl Aves: Galliformes. – Mol. Biol. Evol. 33: 1110–1125.

Hurvich, C. M. and Tsai, C.-L. 1989. Regression and time series model selection in small samples. – Biometrika 76: 297–307.

Kumar, S., Filipski, A. J., Battistuzzi, F. U., Kosakovsky Pond, S. L. and Tamura, K. 2012. Statistics and truth in phylogenomics. – Mol. Biol. Evol. 29: 457–472.

Lim, H. C. and Braun, M J. 2016. High-throughput SNP genotyping of historical and modern samples of five bird species via sequence capture of ultraconserved elements. – Mol. Ecol. Resour. 16: 1204–1223.

Liu K., Warnow, T. J., Holder, M. T., Nelesen, S. M., Yu, J., Stamatakis, A. P. and Linder, C. R. 2011. SATé-II: very fast and accurate simultaneous estimation of multiple sequence alignments and phylogenetic trees. – Syst. Biol. 61: 90–106.

Mariaux, J. and Braun, M. J. 1996. A molecular phylogenetic survey of the nightjars and allies Caprimulgiformes with special emphasis on the potoos Nyctibiidae. – Mol. Phylogenet. Evol. 6: 228–244.

Mayr, G. 2005a. The palaeogene old world potoo Paraprefica Mayr, 1999 aves, Nyctibiidae: its osteology and affinities to the new world preficinae Olson, 1987. – J. Syst. Palaeontol. 3: 359–370.

Mayr, G. 2005b. The paleogene fossil record of birds in Europe. – Biol. Rev. 80: 515–542.

McCormack, J. E., Faircloth, B. C., Crawford, N. G., Gowaty, P. A., Brumfield, R. T. and Glenn, T. C. 2012. Ultraconserved elements are novel phylogenomic markers that resolve placental mammal phylogeny when combined with species-tree analysis. – Genome Res. 22: 46–754.

Prum, R. O., Berv, J. S., Dornburg, A., Field, D. J., Townsend, J. P., Lemmon, E. M. and Lemmon, A. R. 2015. A comprehensive phylogeny of birds (Aves) using targeted next-generation DNA sequencing. – Nature 526: 569–573.

Remsen Jr., J. V., Areta, J. I., Cadena, C. D., Claramunt, S., Jaramillo, A., Pacheco, J. F., Pérez-Emán, J., Robbins, M. B., Stiles, F. G., Stotz, D. F. and Zimmer, K. J. 2016. A classification of the bird species of South America. – American Ornithologists' Union, <www.museum.lsu.edu/~Remsen/SACCBaseline.htm>.

Ricklefs, R. E. 1970. Stage of taxon cycle and distribution of birds on Jamaica, Greater Antilles. – Evolution 24: 475–477.

Salichos, L. and Rokas, A. 2014. Inferring ancient divergences requires genes with strong phylogenetic signals. – Nature 497: 327–331.

Shimodaira, H. 2002. An approximately unbiased test of phylogenetic tree selection. – Syst. Biol. 51: 492–508.

Shimodaira, H. and Hasegawa, M. 1999. Multiple comparisons of log-likelihoods with applications to phylogenetic inference. – Mol. Biol. Evol. 16: 1114–1116.

Stamatakis, A. P. 2014. RAxML ver. 8: a tool for phylogenetic analysis and post-analysis of large phylogenies. – Bioinformatics 30: 1312–1313.

Streicher, J. W., Schulte II, J. A. and Wiens, J. J. 2015. How should genes and taxa be sampled for phylogenomic analyses with missing data? An empirical study in iguanian lizards. – Syst. Biol. 65: 128–145.

Sukumaran, J. and Holder, M. T. 2010. DendroPy: a python library for phylogenetic computing. – Bioinformatics 26: 1569–1571.

Swofford, D. L. 2003. PAUP*. Phylogenetic analysis using parsimony (*and other methods). – Sinauer Associates.

White, N. D., Barrowclough, G. F., Groth, J. G. and Braun, M. J. 2016. A multi-gene estimate of higher-level phylogenetic relationships among nightjars (Aves: Caprimulgidae). – Ornitol. Neotrop. 27: 223–236.

Zerbino, D. 2008. Velvet: algorithms for de novo short read assembly using de Bruijn graphs. – Genome Res. 18: 821–829.

Zwickl, D. J. 2006. Genetic algorithm approaches for the phylogenetic analysis of large biological sequence datasets under the maximum likelihood criterion. – PhD thesis, Univ. of Texas, Austin, TX, USA.